Received: 24 May 2023 | Revised: 20 September 2023 | Accepted: 6 October 2023

DOI: 10.1111/mmi.15182

MINI REVIEW

WILEY

Molecular mapping of virus-infected cells with immunogold and metal-tagging transmission electron microscopy

Martin Sachse [1] | Isabel Fernández de Castro [2] | Raquel Tenorio [2] | Cristina Risco [2]

[1]Centro Nacional de Microbiología/ISCIII, Madrid, Spain

[2]Cell Structure Laboratory, Centro Nacional de Biotecnología, CNB–CSIC, Madrid, Spain

Correspondence
Martin Sachse, Centro Nacional de Microbiología/ISCIII, Majadahonda, Madrid, Spain.
Email: mcrhristoph.sachse@isciii.es

Cristina Risco, Cell Structure Laboratory, Centro Nacional de Biotecnología, CNB–CSIC, Campus de Cantoblanco, Madrid 28049, Spain.
Email: crisco@cnb.csic.es

Funding information
Ministerio de Ciencia e Innovación, Grant/Award Number: RTI2018-094445-B100 MCIU/AEI/FEDER, UE

Abstract

Transmission electron microscopy (TEM) has been essential to study virus–cell interactions. The architecture of viral replication factories, the principles of virus assembly and the components of virus egress pathways are known thanks to the contribution of TEM methods. Specially, when studying viruses in cells, methodologies for labeling proteins and other macromolecules are important tools to correlate morphology with function. In this review, we present the most widely used labeling method for TEM, immunogold, together with a lesser known technique, metal-tagging transmission electron microscopy (METTEM) and how they can contribute to study viral infections. Immunogold uses the power of antibodies and electron dense, colloidal gold particles while METTEM uses metallothionein (MT), a metal-binding protein as a clonable tag. MT molecules build gold nano-clusters inside cells when these are incubated with gold salts. We describe the necessary controls to confirm that signals are specific, the advantages and limitations of both methods, and show some examples of immunogold and METTEM of cells infected with viruses.

KEYWORDS
electron microscopy, immunogold, labeling, METTEM, tomography, virus

1 | INTRODUCTION

Most viruses are rather small, with typical diameters of 10–150 nm, and their morphological study in cells requires the resolution of electron microscopy (EM). Together with the characterization of shape, size, and contacts with cellular structures, labeling and localization of viral and cellular macromolecules are very important to comprehend how viruses use cell materials to build their own structures.

This micro-review presents two labeling methods: Immunogold and METTEM. Immunogold was created more than 50 years ago (Faulk & Taylor, 1971). It uses antibodies as very specific probes to show the localization of two or more different proteins simultaneously. Since the beginning, immunoelectron microscopy has had a major impact in cell biology and virology (Patterson & Verduin, 1983; Sachse et al., 2019; Wolff & Bárcena, 2021). METTEM is a very sensitive technique (Diestra, Fontana, et al., 2009) that uses a small metal-binding protein as a clonable tag to localize protein molecules in cells visualized in two and three dimensions. METTEM has been used in studies about the cell biology of several RNA viruses (Fernández de Castro et al., 2014; Sachse et al., 2019). The principles of METTEM and immunogold are summarized in Figure 1.

Isabel Fernández de Castro and Raquel Tenorio contributed equally to this work.

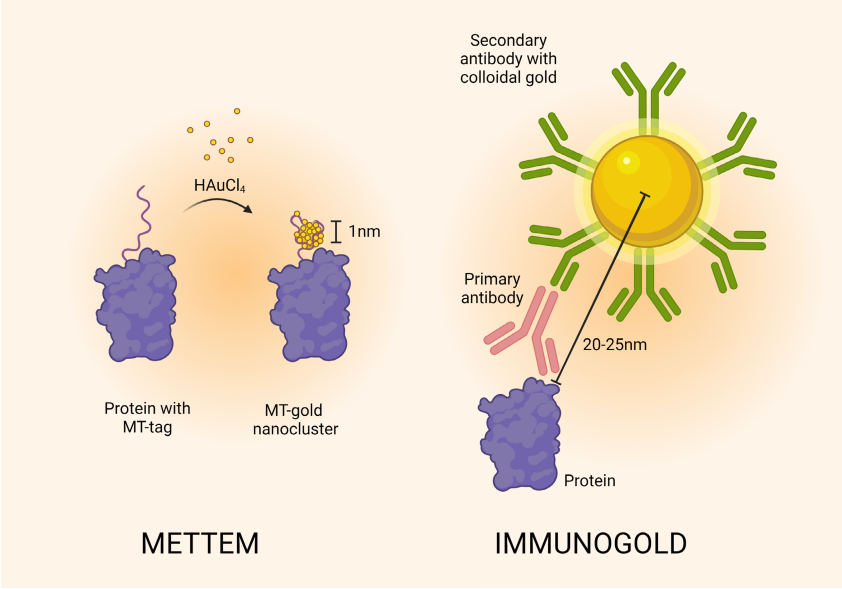

FIGURE 1 Principles of METTEM and Immunogold. For METTEM, cells expressing protein molecules fused with an MT (metallothionein) tag are incubated with a gold salt ($HAuCl_4$). The cys residues within MT will bind gold atoms and make a nanoparticle of ~1 nm that is visible by TEM. For immunogold, samples (viral particles, surface of cells or sections of cells) are incubated with specific primary antibodies that will bind to the epitopes within the macromolecule of interest, and with secondary antibodies conjugated with colloidal gold particles that are visible by TEM. Created with BioRender.com.

2 | ANTIBODIES AND IMMUNOGOLD

For immunolocalization of cellular compounds, any affinity probe can be used. Thus, in the past different probes have emerged: toxins or protein domains for lipid labeling (Möbius et al., 2002; Watt et al., 2002), and lectins for glycosylated proteins (de Lau et al., 2012), but most studies use antibodies for immunolocalization studies. For a successful project, two points are of importance: (A) A sample preparation, which preserves the morphology of the whole sample but does not make the epitope unrecognizable for the antibody. (B) An antibody, which binds specifically and with high affinity to an epitope that has been slightly altered by the sample preparation.

Due to biosafety reasons, sample preparation of cells infected with viruses often starts with chemical fixation by aldehydes to inactivate the virus. Inactivation by aldehyde fixation should preserve the morphology of the sample without major alterations. To do so, buffered solutions of paraformaldehyde (PFA) and glutaraldehyde (GA) are used. PFA has one reactive aldehyde group and reacts with free NH_2 groups, whereas GA has two aldehyde groups and can act as crosslinker. This crosslinking activity results in better morphological preservation but can chemically alter the epitope or hinder the accessibility of it (Takizawa et al., 2003). To avoid the latter, often fixation with PFA alone or a combination of both aldehydes are used, between 2% and 4% PFA with a small amount of 0.05%–0.2% GA. The reaction of the aldehydes with NH_2 groups in the sample produces protons. To avoid acidification during the process of fixation, aldehydes are prepared in buffers with sufficient buffering capacity such as PHEM—60 mM piperazine-*N*,*N*′-bis(2-ethanesulfonic acid [PIPES]), 25 mM (4-[2-hydroxyethyl]-1-piperazineethanesulfonic acid [HEPES], 10 mM EGTA, 2 mM $MgCl_2$), and PIPES or HEPES. After the aldehyde fixation, the sample can be either processed for the Tokuyasu approach (Möbius & Posthuma, 2019; Tokuyasu, 1973) or for an embedding in a resin compatible with immunolabeling such as LR-resins or methacrylate resins (Carlemalm et al., 1982). For the latter, cells are normally post-fixed with a low concentration of uranylacetate and then dehydrated and infiltrated with resins or they can be high pressure frozen and dehydrated and embedded at low temperature by freeze substitution (Schwarz & Humbel, 1989). After polymerization of the resin, thin sections can be cut at room temperature and collected on grids for labeling. For high-pressure freezing, samples without fixation can be processed but as mentioned, biosafety regulations often require inactivation of virus-infected samples.

For the Tokuyasu approach, chemical fixation is mandatory because it makes the plasma membrane permeable for small molecules. This allows to infiltrate the sample with sucrose as a cryo-protectant and afterwards to freeze the samples in liquid nitrogen. The frozen sample is hard enough to cut thin sections with a cryo-microtome. Frozen sections are picked up either with a sucrose solution or a mixture of sucrose and methylcellulose (Liou et al., 1996) and after thawing, deposited on a grid. The labeling is performed on the thawed cryosections. Which approach of sample preparation to choose depends on the question to address and the available equipment. In general, the Tokuyasu approach offers a good visibility of membranes and offers good antigen preservation. However, due to the contrasting, cytosolic ribosomes or cytoskeleton are not visible. Samples embedded in a plastic resin often show less contrast for membranes and lower preservation of antigenicity (Bendayan et al., 1987), but contrasting is less selective compared with the Tokuyasu approach. However, it should be stressed that the best procedure depends on the antigen to be studied.

The other important parameter besides the sample preparation is the antibody. Antibodies are a part of the adaptive immune response of vertebrates (and some invertebrates) to foreign material. Antibodies are made by B cells when they are presented with the native antigen for the antibody they produce. Each B cell is producing only one clone of antibodies. With the immunization of an animal

to produce antibodies, the antigen can be broken down and thus generate several clones of B cells (polyclonal antibody). For a monoclonal antibody, a single B-cell clone is immortalized by fusion with a myeloma cell and can produce antibodies specific for one single epitope.

Independent of the category of an antibody, the variable region of the antibody binds to the epitope with a high affinity. The high-affinity binding of this complex allows immunolabeling since the antibody remains bound with all the washing steps. However, it normally requires some tests whether an antibody really recognizes and binds specific to your epitope of interest (Baker, 2015). One source of cross-reaction for a polyclonal antibody can be an infection of the animal the antibody is made in. It is highly recommended to test the antibody by western blot in the cell line or tissue you want to use. The western blot should show only band(s) that correspond to your protein of interest (Bordeaux et al., 2010). The next step is to determine whether your antibody works with your samples for immunolabeling. A first good and relatively fast test is indirect immunofluorescence (IF) with a negative control. For virus-infected cells, this can be non-infected cells if viral proteins are studied. For cellular markers, either knock out cells or siRNA (small interfering RNA)—treated cells could be used. For siRNA-treated cells, the signal should be reduced on average similar to the knock down levels found with other methods. Alternatively, a treatment which re-localizes your protein of interest can support the specificity of the antibody. In our experience, an antibody which shows no specific signal in IF will not work to label sections for TEM. However, labeling on sections is different compared with labeling for IF: on sections, the epitope is only partial in aqueous environment. Therefore, the conditions of labeling for TEM need to be established with the same controls as for IF to find the right dilution and minimize background because the signal in IF is intensity based, whereas the signal in immunogold labeling is caused by a particulate marker. In early studies, ferritin was used but it was rapidly replaced after the introduction of colloidal gold (Faulk & Taylor, 1971). A colloidal gold particle is either directly adsorbed to the primary antibody, or as now mostly used, to a secondary antibody or protein A. The ability to produce colloidal gold particles with a precise size opened the possibility to label different proteins with different antibodies from different species followed by secondary antibodies-gold or protein A-gold, each with a different size, usually 5, 10, 15, or 20 nm (Slot & Geuze, 1985; Figure 2).

When antibodies work, immunolabeling on sections is a powerful tool to localize proteins at their subcellular compartments. This is illustrated in Figure 2, which shows A549 cells infected with influenza virus, which were prepared for labeling on thawed cryo-sections. The nucleoprotein (NP) of the virus forms with a single strand of negative sense RNA and the viral polymerase, the viral ribonucleoprotein complex (vRNP). The segmented genome is packed in the form of 8 vRNPs at the plasma membrane into the forming viral particle. Labeling for the NP protein shows the presence of it in viral particles at the plasma membrane (Figure 2a). Moreover, label is also present in irregularly coated vesicles (ICVs) with an electron lucent lumen (Figure 2b). Previously, we have shown that these ICVs

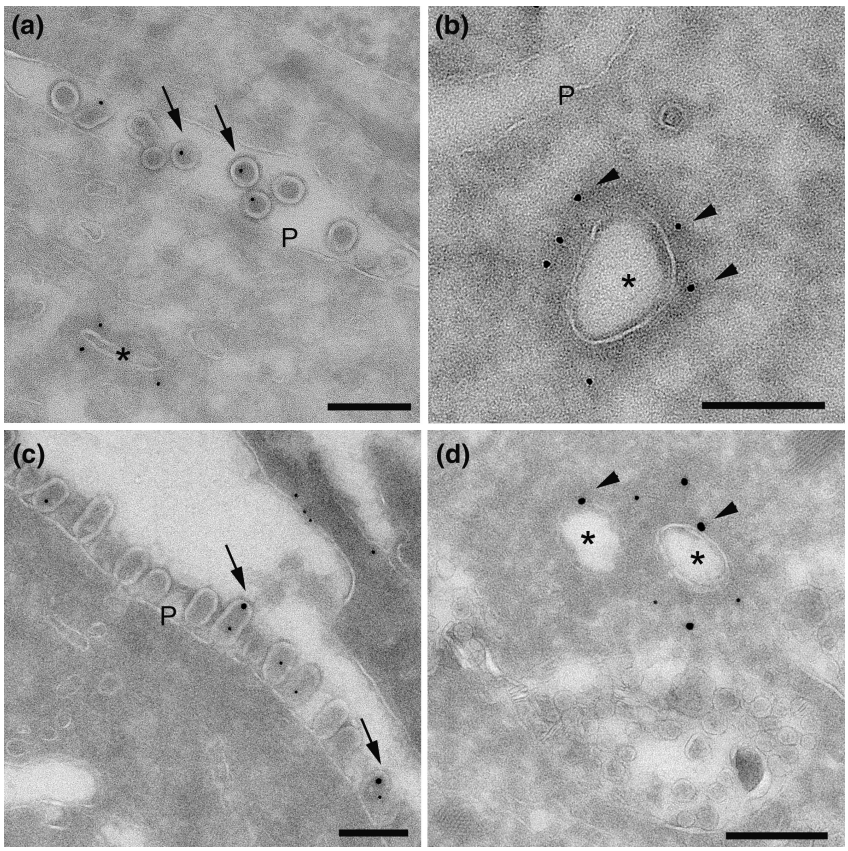

FIGURE 2 Immunogold labeling of influenza virus-infected cells. A549 cells were infected with the influenza virus A/WSN/33 (H1N1) strain and fixed for immuno-EM at 16 h post-infection (hpi). Thawed cryosections were labeled for (a, b) NP (10 nm gold) or (c, d) NP (10 nm gold) and PB2 (15 nm gold). (a) NP is detected in cross-sections of viral particles at the plasma membrane (arrows) and around a tubule with an electron dense coating (asterisk). (b) An ICV (asterisk) in the cytoplasm with label for NP (arrowheads). (c) NP and PB2 co-localize on some cross-sections of viral particles at the plasma membrane (arrows). (d) Two ICVs (asterisks) with label for NP and PB2 in the cytoplasm. P, plasma membrane; scale bars are 200 nm.

represent Rab11 positive transport intermediates of vRNPs to the plasma membrane (de Castro Martin et al., 2017). Double labeling of NP and the subunit PB2 of the viral polymerase showed both proteins co-localizing within VPs (Figure 2c) and on ICVs (Figure 2d), which supports the presence of assembled vRNPs on the ICVs.

3 | METAL-TAGGING TRANSMISSION ELECTRON MICROSCOPY

The use of green fluorescent protein (GFP) as a clonable tag for light microscopy, discovery that received the Nobel Prize in Chemistry (Weiss, 2008), has been a real revolution in cell biology (Cardarelli, 2020; Lippincott-Schwartz et al., 2003; Tsien, 1998). A similar tool for EM has been since long ago the dream of many EM specialists. In 2006, an interesting proposal came from the laboratory of Prof. David DeRosier at Brandeis University. DeRosier's team studied metal-binding proteins such as metallothioneins (MTs) as potential clonable tags for EM (Mercogliano & DeRosier, 2006). MTs are present in some prokaryotes and higher eukaryotes, they are essential for copper (Cu^{+}) and zinc (Zn^{2+}) homeostasis and heavy metal detoxification and can capture a variety of heavy metals (Isani & Carpenè, 2014; Nielson et al., 1985; Scheller et al., 2018; Vašák & Meloni, 2011). It is well known that metal particles are electron dense and can be visible by transmission electron microscopy (TEM), which is also the principle of immunogold (Faulk & Taylor, 1971). Two research articles demonstrated that the idea was correct: when fused with the small metal-binding protein MT, individual protein molecules from *Escherichia coli* incubated with gold salts in vitro built small nanoparticles that were detected by TEM (Mercogliano & DeRosier, 2006, 2007). The mouse MT1 used in their studies is a small protein of 61 aminoacids and a molecular weight of 6 kDa, around four times smaller than GFP. The 20 cysteine (cys) residues of MT1 can bind up to 40 gold atoms by a gold-binding reaction and form a gold nanoparticle ~1 nm in diameter (Mercogliano & DeRosier, 2006). In parallel, the Miyazama group used cadmium salts and a platinum compound instead of gold salts to make the MT-associated nanoparticles and reported positive results when visualizing purified MT-tagged proteins (Fukunaga et al., 2007; Nishino et al., 2007). The challenge was then to use MT as a clonable tag to localize protein molecules inside cells. Optimal results were reported with cultured primary hippocampal neurons expressing a fusion protein of postsynaptic density 95 coupled to three tandem repeats of MT and grown in the presence of cadmium (Cd^{2+}; Fukunaga et al., 2007). In our lab and with the valuable support of Prof. David DeRosier and Dr. Christopher Mercogliano, we established protocols to treat live bacteria that express MT-tagged proteins with gold salts. The results showed the known locations of four different proteins (MBP, AmiC, RecA, and Hfq) together with some other previously unknown locations, as well as changes in the localization and state of aggregation of protein molecules depending on the physiological state of the cells (Diestra, Cayrol, et al., 2009; Diestra, Fontana, et al., 2009). Then we moved to yeast and mammalian cells and the final name of our technique was established as METTEM (de Castro Martin et al., 2017; Fernández de Castro et al., 2014, 2017; Risco et al., 2012). Four different gold salts were tested, AuCl, $AuCl_3$, aurothiomalate, and $HAuCl_4$, being the latter the less toxic and the most adequate for METTEM of live mammalian cells. Incubation of live cells with gold salts has to be short, around 5–10 min, to avoid cell toxicity. In mammalian cells, gold salts reach intracellular locations within minutes, a time span too brief for cytopathology to occur (Risco et al., 2012). Nonetheless, concentration of the gold salt and time of incubation have to be adjusted for each cell type using a toxicity test such as trypan blue exclusion. Protocols that include incubation of cells with gold salts after fixation and embedding or during the freeze-substitution process have been developed to avoid toxicity issues (Morphew et al., 2015). Visualization of MT-gold nanoparticles is done by TEM of ultra-thin (50–70 nm), unstained sections of methacrylate resins such as Lowicryl (Risco et al., 2012) or acrylic resins, such as LRWhite (Fernández de Castro et al., 2014). Stained epoxy resin sections can be used as well, but in this case, a step of silver enhancement or a gold-enhancing solution are needed to increase the size of MT-gold nano-particles (de Castro Martin et al., 2017; Morphew et al., 2015; Figure 3). Because labeling can be done in whole, live cells, the sensitivity of the method is often higher than that provided by antibodies on sections (Risco et al., 2012). Like with any other labeling method, specificity of signals has to be demonstrated with adequate controls. Although unspecific background produced by endogenous, cellular MTs is negligible (Risco et al., 2012), potential binding of gold atoms to other metal-binding molecules and structures in the cell has to be investigated. When localizing viral proteins, the adequate control would be studying non-infected cells treated with gold salts. In the case of MT-tagged cellular proteins, transfected cells expressing untagged versions of the proteins and incubated with gold salts will be the control to use. TEM of serial sections covering the whole cell volume should be done to confirm the absence of unspecific background. Moreover, immunogold labeling with antibodies specific for MT or the tagged protein is very important to validate the results of METTEM and to confirm the identity of the MT-gold particles detected in cells. When possible, correlative light and electron microscopy of GFP and MT double-tagged-proteins provides an additional verification of the specificity of MT-gold labeling, allowing the detection of the same macromolecules with different spatial resolutions (Fernández de Castro et al., 2014; Risco et al., 2012). METTEM is a method for single labeling only, and it needs to be combined with immunogold for localizing two or more proteins. METTEM is compatible with a variety of sample processing methods, such as negative staining of single particles, conventional embedding of cells in resins, high-pressure freezing and freeze substitution, cryo-EM, and cryo-electron microscopy of vitreous sections (CEMOVIS; Bouchet-Marquis et al., 2012; Diestra, Fontana, et al., 2009; Fukunaga et al., 2012; Hirabayashi et al., 2014; Mercogliano & DeRosier, 2007; Morphew et al., 2015; Nishino et al., 2007; Zhou et al., 2012). METTEM can be combined with three-dimensional imaging, such electron tomography (Bouchet-Marquis et al., 2012; Diestra, Fontana, et al., 2009;

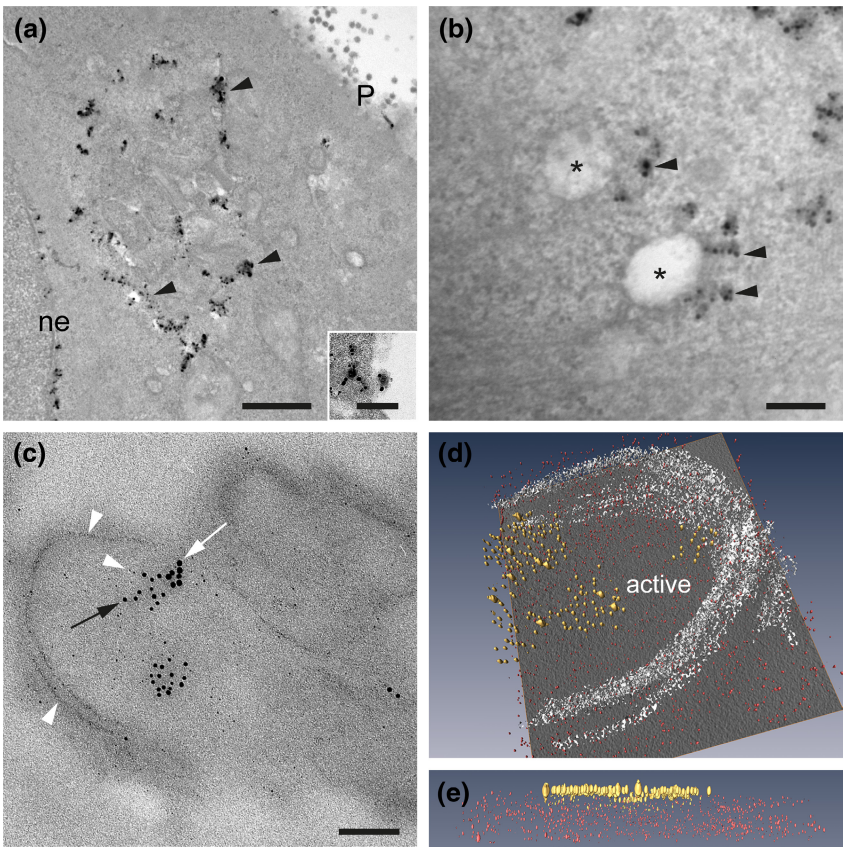

FIGURE 3 METTEM of influenza virus-infected cells and METTEM combined with immunogold of TBSV-infected cells. (a, b) A549 cells were infected with the influenza recombinant virus WSN-PB2-MT, treated for 30 min with 0.25 mM $HAuCl_4$ at 8 hpi, fixed with aldehydes and incubated with silver to increase the diameter of gold nanoclusters built by the MT tag. Cells were post-fixed with osmium tetroxide, dehydrated, embedded in epoxy resin, sectioned, stained, and studied by TEM. (a) Cell showing MT-labeled vRNPs at the nuclear envelope (ne), ER (arrowheads) and close to the plasma membrane (P). The inset shows an MT-gold-labeled viral particle on the cell surface. (b) MT-gold signal associated with vRNPs (arrowheads) on the periphery of irregularly coated vesicles (ICVs, asterisks). (c–e) TBSV replication organelles in yeast studied by immunogold and METTEM. Yeast spheroplasts were incubated for 75 min with 2 mM $HAuCl_4$, fixed with aldehydes, dehydrated, and embedded in LR-White acrylic resin (c) Ultra-thin, non-stained section of a yeast cell expressing HA-tagged Vps4p (detected with an anti-HA antibody and 10 nm gold particles, white arrow), replicating TBSV repRNA (detected with an anti-dsRNA antibody and 5 nm gold particles, black arrow) and MT-tagged p33 (~1 nm gold nano-clusters associated to MT, white arrowheads). P33, dsRNA and Vps4p colocalize in the same compartment. (d, e) Electron tomography and 3D reconstructions of a TBSV replication organelle. Thick sections were processed by immunogold labeling with an antibody against dsRNA and a colloidal gold conjugate (yellow). (d) Frontal view of a tomogram. The MT-tagged p33 molecules are detected with the ~1 nm gold nano-clusters associated with MT (pink) and the ER membranes were segmented in white. The antibodies label an active domain within the replication organelle that is surrounded by ER membranes. (e) Lateral view of the tomogram in (d) showing antibodies bound to their antigens on the section surface (yellow), whereas p33 molecules (pink) were detected inside the section. Scale bar for (a) is 1 μm; for the inset and (b), it is 200 nm; and for (c), it is 100 nm. Panels (a and b) modified from de Castro et al. (2017). Panel (c) modified from Barajas et al. (2014); panels (d, e) modified from Fernández de Castro et al. (2017).

Fernández de Castro et al., 2017; Hirabayashi et al., 2014; Morphew et al., 2015).

4 | METTEM AND IMMUNOGOLD OF CELLS INFECTED WITH VIRUSES

METTEM has been applied to study the intracellular distribution of rubella virus replicase and capsid proteins (Risco et al., 2012). The results of this study helped to characterize the biogenesis of rubella virus factory that starts with the accumulation of replicase molecules at the plasma membrane and their transport by endocytosis to modified lysosomes that become the viral replication organelles (Risco et al., 2012). In reovirus-infected cells, an MT-tagged version of the μNS viral non-structural protein was localized to strangled endoplasmic reticulum (ER) cisternae and in small vesicles which is compatible with the μNS—mediated fragmentation of the ER observed by confocal microscopy early in infection (Tenorio et al., 2018). This ER remodeling produces collections of tubules and vesicles that form the viral replication factory (Tenorio et al., 2018). Thanks to METTEM, the transport pathway of influenza virus ribonucleoproteins (vRNPs) from the nucleus to the

plasma membrane was identified (de Castro Martin et al., 2017). Influenza vRNPs abandon the nucleus through nuclear pores and once in the cytosol, they associate with modified ER cisternae (Figure 3a). As described in Section 2, the ICVs are formed in influenza virus-infected cells (Figures 2b,d and 3b). METTEM, immunogold and morphological analysis suggested that ICVs emerge from ER cisternae with vRNPs attached, before carrying them to the plasma membrane. ICVs are a new kind of organelle created by influenza virus, they have markers of both the ER and recycling endosomes and their formation requires a functional Rab11 GTPase (de Castro Martin et al., 2017).

Tombusviruses are small RNA viruses that infect plants and are used as model viruses to study virus–host interactions using yeast (*Saccharomyces cerevisiae*; Nagy et al., 2014; Nagy & Feng, 2021). The replication organelles of the tombusvirus tomato bushy stunt virus (TBSV), have been visualized in yeast with METTEM and immunogold (Barajas et al., 2014; Fernández de Castro et al., 2017). MT-tagged p33 viral replicase protein molecules were localized in yeast intracellular membranes (Figure 3c). The identity of the replication organelle membranes was confirmed with immunogold labeling using antibodies specific for the ER (Figure 3c), whereas antibodies specific for double-stranded RNA (dsRNA), a marker of viral replication, spotted regions where the replicase molecules are active (Figure 3c,d; Barajas et al., 2014; Fernández de Castro et al., 2017; Sachse et al., 2022). Electron tomography showed the distribution of TBSV p33 replicase molecules in three dimensions (Figure 3d). Lateral views of the tomogram show the antibodies and colloidal gold particles bound to the section surface, while MT-gold-tagged p33 molecules are inside the section (Figure 3e). These results demonstrate that the combination of immunogold and METTEM to study viruses in cells can be very informative (Sachse et al., 2018) because together with the fine localization of the molecules of interest, we can explore their functional state and identify the cell compartments used and transformed by viruses.

5 | CONCLUSIONS

Immunogold has been in place since 1971 and its contribution to the characterization of many aspects of viral infections is remarkable. Protocols for using MT as a clonable tag for TEM of biological samples were first reported in 2006. Subsequently, MT and METTEM have been applied to study a variety of structures assembled by Rubella virus, the human reovirus, influenza virus, and a tombusvirus. In general, these methods are applicable to study the molecular organization of microbes and the principles that govern host–pathogen interactions (Table 1). The powerful combination of Immunogold and METTEM shows where macromolecules go inside cells, changes in their organization and their functional status. Future technical challenges will include the development of protocols to combine METTEM and immunogold with the Tokuyasu method for simultaneous labeling of multiple macromolecules. Using METTEM together with high-resolution cryo-EM of cells such as CEMOVIS and cryo-electron tomography of cryo-lamella, will offer new opportunities to study viral macromolecular structures in their native state and in their natural environment.

AUTHOR CONTRIBUTIONS

Cristina Risco: Conceptualization; funding acquisition; writing – original draft; writing – review and editing; methodology; supervision; resources; validation; investigation. **Martin Sachse:** Conceptualization; writing – original draft; writing – review and editing; investigation; methodology; validation; supervision. **Isabel Fernández de Castro:** Conceptualization; investigation; writing – review and editing; methodology; validation. **Raquel Tenorio:**

TABLE 1 Principles, properties, advantages, and applications of Immunogold and METTEM for labeling macromolecules in biological samples.

	Immunogold	METTEM
Principles	Specific primary antibodies and secondary antibodies conjugated with colloidal gold particles	Metal-binding protein as a clonable tag that builds a ~1 nm gold nanocluster when incubated with gold salts
Specificity	Very high with the optimal dilutions of antibodies	High. Confirmation with immunogold is recommended
Sensitivity	High. Restricted to the epitopes exposed on the structure or section surface	Very high. Proteins in the whole cell volume can be labeled
Resolution	High. The colloidal gold marker is visualized at ~10–25 nm from the labeled epitope	Very high. Proteins are labeled with a ~1 nm MT-gold nanocluster attached to the protein molecule
Multiple labeling	Yes, two or more different macromolecules can be labeled simultaneously with colloidal gold conjugates of different sizes	No, only single labeling is possible
Labeling in 3D	Can be combined with 3D EM only for macromolecules on the surface of cells or viruses	Can be combined with 3D EM for proteins inside or on the surface of cells and viruses
Toxicity	NA	For labeling live cells, toxicity should be under control. For protocols with fixed cells, NA
Applications	Labeling macromolecules in viruses, cells, tissues, and whole organisms	Labeling proteins in viruses and cells. Protocols for tissues have not been developed

Conceptualization; investigation; methodology; validation; writing – review and editing.

ACKNOWLEDGMENTS

This work has been funded by grant RTI2018-094445-B100 (MCIU/AEI/FEDER, UE) from the Ministry of Science and Innovation of Spain (C.R.). We are grateful to Ms. Sara Y. Fernández-Sánchez for critically reading the manuscript. We acknowledge support of the publication fee by the CSIC Open Access Publication Support Initiative through its Unit of Information Resources for Research (URICI).

CONFLICT OF INTEREST STATEMENT

The authors declare no conflict of interest.

DATA AVAILABILITY STATEMENT

Data sharing is not applicable to this article as no new data were created or analyzed in this study.

ETHICS STATEMENT

This review article refers to published data from the communicating authors' laboratories. No data were collected using human or animal subjects. All data were collected following laboratory and biosafety policies of CSIC and ISCIII. Antibodies used in this study are available commercially or were published previously. The authors prepared the manuscript text without the use of Artificial Intelligence systems that generate content in an automated manner.

ORCID

Martin Sachse https://orcid.org/0000-0001-5981-9166
Isabel Fernández de Castro https://orcid.org/0000-0002-5388-8934
Raquel Tenorio https://orcid.org/0000-0003-0547-155X
Cristina Risco https://orcid.org/0000-0001-7501-5934

REFERENCES

Baker, M. (2015) Reproducibility crisis: blame it on the antibodies. *Nature*, 521, 274–276. Available from: https://doi.org/10.1038/521274a

Barajas, D., Martín, I.F.D.C., Pogany, J., Risco, C. & Nagy, P.D. (2014) Noncanonical role for the host Vps4 AAA+ ATPase ESCRT protein in the formation of tomato bushy stunt virus replicase. *PLoS Pathogens*, 10(4), e1004087. Available from: https://doi.org/10.1371/journal.ppat.1004087

Bendayan, M., Nanci, A. & Kan, F.W. (1987) Effect of tissue processing on colloidal gold cytochemistry. *Journal of Histochemistry and Cytochemistry*, 35, 983–996. Available from: https://doi.org/10.1177/35.9.3302022

Bordeaux, J., Welsh, A., Agarwal, S., Killiam, E., Baquero, M., Hanna, J. et al. (2010) Antibody validation. *BioTechniques*, 48, 197–209. Available from: https://doi.org/10.2144/000113382

Bouchet-Marquis, C., Pagratis, M., Kirmse, R. & Hoenger, A. (2012) Metallothionein as a clonable high-density marker for cryo-electron microscopy. *Journal of Structural Biology*, 177, 119–127. Available from: https://doi.org/10.1016/j.jsb.2011.10.007

Cardarelli, F. (2020) Back to the future: genetically encoded fluorescent proteins as inert tracers of the intracellular environment. *International Journal of Molecular Sciences*, 21, 4164.

Carlemalm, E., Garavito, R.M. & Villinger, W. (1982) Resin development for electron microscopy and an analysis of embedding at low temperature. *Journal of Microscopy*, 126, 123–143. Available from: https://doi.org/10.1111/j.1365-2818.1982.tb00362.x

de Castro Martin, I.F., Fournier, G., Sachse, M., Pizarro-Cerda, J., Risco, C. & Naffakh, N. (2017) Influenza virus genome reaches the plasma membrane via a modified endoplasmic reticulum and Rab11-dependent vesicles. *Nature Communications*, 8, 1396. Available from: https://doi.org/10.1038/s41467-017-01557-6

de Lau, W., Kujala, P., Schneeberger, K., Middendorp, S., Li, V.S., Barker, N. et al. (2012) Peyer's patch M cells derived from Lgr5(+) stem cells require SpiB and are induced by RankL in cultured "miniguts". *Molecular and Cellular Biology*, 32, 3639–3647. Available from: https://doi.org/10.1128/MCB.00434-12

Diestra, E., Cayrol, B., Arluison, V. & Risco, C. (2009) Cellular electron microscopy imaging reveals the localization of the Hfq protein close to the bacterial membrane. *PLoS One*, 4(2), e8301. Available from: https://doi.org/10.1371/journal.pone.0008301

Diestra, E., Fontana, J., Guichard, P., Marco, S. & Risco, C. (2009) Visualization of proteins in intact cells with a clonable tag for electron microscopy. *Journal of Structural Biology*, 165, 157–168. Available from: https://doi.org/10.1016/j.jsb.2008.11.009

Faulk, W.P. & Taylor, G.M. (1971) An immunocolloid method for the electron microscope. *Immunochemistry*, 8, 1081–1083. Available from: https://doi.org/10.1016/0019-2791(71)90496-4

Fernández de Castro, I., Fernández, J.J., Barajas, D., Nagy, P.D. & Risco, C. (2017) Three-dimensional imaging of the intracellular assembly of a functional viral RNA replicase complex. *Journal of Cell Science*, 130(1), 260–268. Available from: https://doi.org/10.1242/jcs.181586

Fernández de Castro, I., Sanz-Sánchez, L. & Risco, C. (2014) Metallothioneins for correlative light and electron microscopy. *Methods in Cell Biology*, 124, 55–70. Available from: https://doi.org/10.1016/B978-0-12-801075-4.00003-3

Fukunaga, Y., Higashihara, A., Nishino, Y., Yasunaga, T., Jin, M. & Miyazawa, A. (2012) Enhanced detection efficiency of genetically encoded tag allows the visualization of monomeric proteins by electron microscopy. *Journal of Electron Microscopy*, 61(4), 229–236. Available from: https://doi.org/10.1093/jmicro/dfs043

Fukunaga, Y., Hirase, A., Kim, H., Wada, N., Nishino, Y. & Miyazawa, A. (2007) Electron microscopic analysis of a fusion protein of post-synaptic density-95 and metallothionein in cultures hippocampal neurons. *Journal of Electron Microscopy*, 56(4), 119–129. Available from: https://doi.org/10.1093/jmicro/dfm027

Hirabayashi, A., Fukunaga, Y. & Miyazawa, A. (2014) Structural analysis of the PSD-95 cluster by electron tomography and CEMOVIS: a proposal for the application of the genetically encoded metallothionein tag. *Microscopy*, 63(3), 227–234. Available from: https://doi.org/10.1093/jmicro/dfu006

Isani, G. & Carpenè, E. (2014) Metallothioneins, unconventional proteins from unconventional animals: a long journey from nematodes to mammals. *Biomolecules*, 4(2), 435–457. Available from: https://doi.org/10.3390/biom4020435

Liou, W., Geuze, H.J. & Slot, J.W. (1996) Improving structural integrity of cryosections for immunogold labeling. *Histochemistry and Cell Biology*, 106, 41–58. Available from: https://doi.org/10.1007/BF02473201

Lippincott-Schwartz, J., Gardel, M.L., Shin, J.H., Mackintosh, F.C., Mahadevan, L., Matsudaira, P. et al. (2003) Development and use of fluorescent protein markers in living cells. *Science*, 300, 87–91.

Mercogliano, C.P. & DeRosier, D.J. (2006) Gold nanocluster formation using metallothionein: mass spectrometry and electron microscopy. *Journal of Molecular Biology*, 355(2), 211–223. Available from: https://doi.org/10.1016/j.jmb.2005.10.026

Mercogliano, C.P. & DeRosier, D.J. (2007) Concatenated metallothionein as a clonable gold label for electron microscopy. *Journal of Structural*

Biology, 160(1), 70–82. Available from: https://doi.org/10.1016/j.jsb.2007.06.010

Möbius, W., Ohno-Iwashita, Y., van Donselaar, E.G., Oorschot, V.M., Shimada, Y., Fujimoto, T. et al. (2002) Immunoelectron microscopic localization of cholesterol using biotinylated and non-cytolytic perfringolysin O. *Journal of Histochemistry and Cytochemistry*, 50, 43–55. Available from: https://doi.org/10.1177/002215540205000105

Möbius, W. & Posthuma, G. (2019) Sugar and ice: immunoelectron microscopy using cryosections according to the Tokuyasu method. *Tissue and Cell*, 57, 90–102. Available from: https://doi.org/10.1016/j.tice.2018.08.010

Morphew, M.K., O'Toole, E.T., Page, C.L., Pagratis, M., Giddings, T., Gardner, J.M. et al. (2015) Metallothionein as a clonable tag for protein localization by electron microscopy of cells. *Journal of Microscopy*, 260(1), 20–29. Available from: https://doi.org/10.1111/jmi.12262

Nagy, P.D. & Feng, Z. (2021) Tombusviruses orchestrate the host endomembrane system to create elaborate membranous replication organelles. *Current Opinion in Virology*, 48, 30–41. Available from: https://doi.org/10.1016/j.coviro.2021.03.007

Nagy, P.D., Pogany, J. & Lin, Y.J. (2014) How yeast can be used as a genetic platform to explore virus-host interactions: from 'omics' to functional studies. *Trends in Microbiology*, 22, 309–316. Available from: https://doi.org/10.1016/j.tim.2014.02.003

Nielson, K.B., Atkin, C.L. & Winge, D.R. (1985) Distinct metal-binding configurations in metallothionein. *Journal of Biological Chemistry*, 260, 5342–5350.

Nishino, Y., Yasunaga, T. & Miyazawa, A. (2007) A genetically encoded metallothionein tag enabling efficient protein detection by electron microscopy. *Journal of Electron Microscopy*, 56(3), 93–101. Available from: https://doi.org/10.1093/jmicro/dfm008

Patterson, S. & Verduin, B.J. (1983) Applications of immunogold labeling in animal and plant virology. *Archives in Virology*, 97(1–2), 1–26. Available from: https://doi.org/10.1007/BF01310730

Risco, C., Sanmartín-Conesa, E., Tzeng, W.-P., Frey, T.K., Seybold, V. & de Groot, R.J. (2012) Specific, sensitive, high-resolution detection of protein molecules in eukaryotic cells using metal-tagging transmission electron microscopy. *Structure*, 20, 759–766. Available from: https://doi.org/10.1016/j.str.2012.04.001

Sachse, M., Fernández de Castro, I., Fournier, G., Naffakh, N. & Risco, C. (2018) Metal-tagging transmission electron microscopy and immunogold labeling on Tokuyasu cryosections to image influenza A virus ribonucleoprotein transport and packaging. *Methods in Molecular Biology*, 1836, 281–301. Available from: https://doi.org/10.1007/978-1-4939-8678-1_14

Sachse, M., Fernández de Castro, I., Tenorio, R. & Risco, C. (2019) The viral replication organelles within cells studied by electron microscopy. *Advances in Virus Research*, 105, 1–33. Available from: https://doi.org/10.1016/bs.aivir.2019.07.005

Sachse, M., Tenorio, R., Fernández de Castro, I., Muñoz-Basagoiti, J., Perez-Zsolt, D., Raïch-Regué, D. et al. (2022) Unraveling the antiviral activity of plitidepsin against SARS-CoV-2 by subcellular and morphological analysis. *Antiviral Research*, 200, 105270. Available from: https://doi.org/10.1016/j.antiviral.2022.105270

Scheller, J.S., Irvine, G.W. & Stillman, M.J. (2018) Unravelling the mechanistic details of metal binding to mammalian metallothioneins from stoichiometric, kinetic, and binding affinity data. *Dalton Transactions*, 47, 3613. Available from: https://doi.org/10.1039/c7dt03319b

Schwarz, H. & Humbel, B.M. (1989) Influence of fixatives and embedding media on immunolabelling of freeze-substituted cells. *Scanning Microscopy. Supplement*, 3, 57–63.

Slot, J.W. & Geuze, H.J. (1985) A new method of preparing gold probes for multiple-labeling cytochemistry. *European Journal of Cell Biology*, 38, 87–93.

Takizawa, T., Anderson, C.L. & Robinson, J.M. (2003) A new method to enhance contrast of ultrathin cryosections for immunoelectron microscopy. *Journal of Histochemistry and Cytochemistry*, 51, 31–39. Available from: https://doi.org/10.1177/002215540305100105

Tenorio, R., Fernández de Castro, I., Knowlton, J.J., Zamora, P.F., Lee, C.H., Mainou, B.A. et al. (2018) Reovirus σNS and μNS proteins remodel the endoplasmic reticulum to build replication neo-organelles. *mBio*, 9(4), e01253-18. Available from: https://doi.org/10.1128/mBio.01253-18

Tokuyasu, K.T. (1973) A technique for ultracryotomy of cell suspensions and tissues. *Journal of Cell Biology*, 57, 551–565. Available from: https://doi.org/10.1083/jcb.57.2.551

Tsien, R.Y. (1998) The green fluorescent protein. *Annual Review of Biochemistry*, 67, 509–544.

Vašák, M. & Meloni, G. (2011) Chemistry and biology of mammalian metallothioneins. *Journal of Biological Inorganic Chemistry*, 16, 1067–1078. Available from: https://doi.org/10.1007/s00775-011-0799-2

Watt, S.A., Kular, G., Fleming, I.N., Downes, C.P. & Lucocq, J.M. (2002) Subcellular localization of phosphatidylinositol 4,5-bisphosphate using the pleckstrin homology domain of phospholipase C delta1. *Biochemical Journal*, 363, 657–666. Available from: https://doi.org/10.1042/0264-6021:3630657

Weiss, P.S. (2008) 2008 Nobel prize in chemistry: green fluorescent protein, its variants and implications. *ACS Nano*, 2(10), 1977. Available from: https://doi.org/10.1021/nn800671h

Wolff, G. & Bárcena, M. (2021) Multiscale electron microscopy for the study of viral replication organelles. *Viruses*, 13, 197. Available from: https://doi.org/10.3390/v13020197

Zhou, Q., Sun, S., Tai, P. & Sui, S.-F. (2012) Structural characterization of the complex of SecB and metallothionein-labeled proOmpA by cryo-electron microscopy. *PLoS One*, 7(10), e47015. Available from: https://doi.org/10.1371/journal.pone.0047015

How to cite this article: Sachse, M., de Castro, I.F., Tenorio, R. & Risco, C. (2023) Molecular mapping of virus-infected cells with immunogold and metal-tagging transmission electron microscopy. *Molecular Microbiology*, 00, 1–8. Available from: https://doi.org/10.1111/mmi.15182